Reactions over catalysts confined in carbon nanotubes

Xiulian Pan and Xinhe Bao*

Received (in Cambridge, UK) 30th June 2008, Accepted 4th September 2008
First published as an Advance Article on the web 14th October 2008
DOI: 10.1039/b810994j

We review a new concept for modifying the redox properties of transition metals *via* confinement within the channels of carbon nanotubes (CNTs), and thus tuning their catalytic performance. Attention is also devoted to novel techniques for homogeneous dispersion of metal nanoparticles inside CNTs since these are essential for optimization of the catalytic activity.

1. Introduction

Carbon is an important support material and has been widely used in chemical industry to disperse precious metal catalysts as small particles in order to obtain a higher number of catalytically active metal atoms.[1] Carbon nanotubes (CNTs), which were only discovered in 1991, are considered to be a promising alternative to the widely used activated carbons due to their unique properties.[2–5] They possess very good electrical conductivity, mechanical strength, thermal stability and hydrogen storage capability.[2,3] Studies have shown the benefits of using CNTs as supports for dispersion of transition metal catalysts on their outer surface in hydrogen involving reactions such as hydrogenation and fuel cell electrocatalytic reactions.[4–8] Improved activities and/or product selectivities have often been reported compared to *e.g.* Al_2O_3, SiO_2 and even activated carbon supported catalysts. Recent reviews have summarized significant progress in this field.[5,6]

State Key Laboratory of Catalysis, Dalian Institute of Chemical Physics, Zhongshan Road 457, Dalian, 116023, China. E-mail: panxl@dicp.ac.cn. E-mail: xhbao@dicp.ac.cn; Fax: 86 411 8469 4447; Tel: 86 411 8437 9128

What distinguishes CNTs from other carbon materials is their nanochannels formed by graphene layers.[2,3] The channel size ranges from as small as less than one nanometer up to a hundred nanometers in diameter, which may provide an intriguing confinement environment for nanocatalysts and catalytic reactions. However, this has not been studied until recently.

On the other hand, zeolites and other mesoporous materials with a periodic pore structure of similar diameters *e.g.* SBA-15 have been extensively applied in catalysis.[9,10] Their small pores restrict the growth of catalyst particles and prevent sintering at high temperatures. Therefore, the well defined nanochannels of CNTs are expected to provide a similar space restriction for nanocatalysts. This restriction has been reported to influence the structures and other properties of substances, which have been introduced into the CNT channels, *e.g.* fullerenes and its derivatives, water, alkali metals and halides.[11–14] For example, the lattice of KI crystals is distorted[12] and water molecules form a layered cylindrical structure with hydrogen-bonding in a heptagonal ring,[13] which do not exist in the bulk phase.

In addition, inside such small channels the interactions of reactant and product molecules with the pore walls become increasingly important and finally dominate compared to the intermolecular interaction. This may alter the thermodynamics

Xiulian Pan

Xiulian Pan received her PhD from Dalian Institute of Chemical Physics of the Chinese Academy of Sciences in 2001 after carrying out a thesis on development of palladium hollow fiber membranes for hydrogen separation and membrane catalysis under the guidance of Prof. Guoxing Xiong. After two years as a postdoctoral fellow at the Fraunhofer Institute of Interfacial Engineering and Biotechnology in Stuttgart, Germany, she joined Prof. Xinhe Bao's group at Dalian Institute of Chemical Physics as an associate professor at the end of 2003. Her current research interests center on reactions over catalysts confined in one-dimensional nanoporous systems, especially carbon nanotubes and mesoporous silicas.

Xinhe Bao

Xinhe Bao received his PhD in Physical Chemistry from Fudan University in China in 1987. He moved to Germany in 1989 and worked as an Alexander von Humboldt Research Fellow in the Frize-Haber institute, hosted by Prof. Ertl. In 1995, he came back to China and joined the Dalian Institute of Chemical Physics (DICP) as a full Professor. His research activities focus on the fundamental study of catalysis, including development of new catalysts and novel catalytic processes related to energy. Currently, much attention is paid on "nanocatalysis" with emphasis on the development of science and techniques to assemble and to stabilize nano-structured particles using porous materials and carbon nanotubes.

of a reaction.[15] Furthermore, if metal catalysts are introduced inside nanotubes, a unique metal–support interaction may result because of the deformed sp^2 hybridization electron structure of the graphene walls. Deviation from planarity causes π-electron density to shift from the concave inner to the convex outer surface, leading to an electron potential difference between inside and outside of CNTs.[16–19] Thus, the metal–support interaction inside CNTs may be different from the case with catalysts located on the exterior surfaces of CNTs.[20,21] For example, theoretical simulation shows that transition metal atoms interact with CNT walls differently from that with graphite layers with regard to bonding sites, magnetic moments and charge-transfer directions.[22] This opens up an opportunity to tune the catalytic performance *via* confinement inside CNTs.[23,24]

Here we focus on a new concept, *i.e.* reactions over CNT-confined catalysts reviewing recent theoretical and experimental advances in this field. Since homogeneous dispersion of metal nanocatalysts particularly inside small CNTs is essential to achieve optimized catalytic activity and is still a great challenge for experimental study, novel techniques of filling nanotubes with metal catalysts are discussed first. Then we show that the redox properties of catalysts can be tuned through the metal–support interaction inside CNTs. Consequently their catalytic behavior is modified with respect to the catalysts supported on the CNT exterior surfaces.

2. Tailoring of CNTs for catalytic applications

2.1 Techniques of filling CNTs

The one-dimensional tubular morphology of CNTs has triggered wide interest in fabricating composite materials with foreign substances inserted in the channels. Several techniques have been developed for filling CNTs. For example, metals have been introduced inside CNTs during arc discharge growth of nanotubes.[25,26] Both carbon and metal sources are passed simultaneously through the arc discharge. The metals crystallize on the cathode and CNTs grow around them. This process is usually operated at rather high temperatures. Thus the confined metals are frequently accompanied by formation of their carbides as byproducts. In addition, the resulting metals are often encapsulated completely inside the carbon shell[25,26] and will be inaccessible to reactants in catalytic reactions.

Transition metals such as Fe and Co have been inserted in the CNT channels by vapor deposition of volatile complexes, *e.g.* ferrocene and cobaltocene.[27–29] The process usually involves evacuation of the CNT channels followed by evaporation and decomposition of the metallocenes to form metals and carbon inside CNTs. However, a great deal of metal complexes also deposit on the CNT exterior surfaces, which need to be removed carefully. This is inconvenient for controlling the metal loadings.

Due to the tubular morphology of CNTs, liquids can be sucked into the channels because of the capillary forces. Filling depends on the pressure difference across the liquid–vapor interface, which is related to the surface tension of the liquid and the contact angle between the liquid and the CNT pore walls.[30,31] It has been predicted that liquids with a surface tension below 100–200 mN m^{-1} can wet CNTs and can be filled inside the channels at atmospheric pressure through an open end.[30]

Ajayan *et al.* first reported filling MWNTs with low melting metals such as lead and bismuth in the presence of oxygen.[32] Through oxidation of carbon by oxygen the nanotubes were opened and the liquid was drawn in to the channels by the capillary forces. Ugarte *et al.* introduced silver into CNTs using molten salt $AgNO_3$ followed by decomposition under the electron microscope beam.[17] Recently, Chernysheva *et al.* inserted molten CuI in nanotubes under vacuum.[33] This technique is limited to metals and metal salts with low melting points.

However, most of the filled materials resulting from the above techniques often exist in the form of nanowires, rods or particles mixed with wires and rods.[25,26,32] Such inhomogeneous dispersion of catalysts with varying dimensions is not preferred for catalytic reactions with respect to activity and selectivity. Furthermore, the CNT channels seem to be frequently blocked by these wires or rods, which will cause the metals at the inner part of the channels to be not easily accessible to reactants and significant diffusion resistances for products out of the channels.

Wet chemistry methods using inorganic or organic solutions containing metal precursors appear to be simpler and more versatile for filling CNTs.[34–36] They are suitable for most metals and metal oxides and are more likely to achieve homogeneously distributed nanoparticles.[36] Tsang *et al.* introduced NiO and UO_{2+x} crystals inside CNTs by refluxing nickel nitrate and uranyl nitrate, respectively, in nitric acid solution followed by heat-treatment.[34] Chu *et al.* reported that $AgNO_3$ and $AuCl_3$ were introduced in nanotubes by stirring a mixture of the previously opened nanotubes with an excess concentrated aqueous solution of metal salts.[35] For example, Fig. 1 shows Ag crystals inside CNTs obtained by decomposition of the incorporated $AgNO_3$ upon heat-treatment.[35]

However, difficulties are often encountered during filling[17,31,36] and the filling efficiency has been low so far. Very often only a small amount of tubes are filled and a relatively large portion of metals are deposited on the outside of CNTs. In particular filling nanotubes with a diameter smaller than 10 nm, which should be most interesting for confining

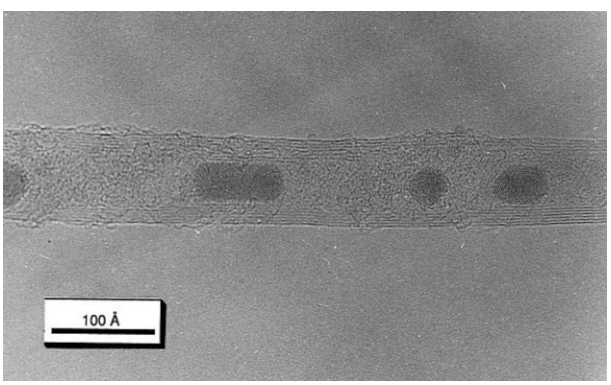

Fig. 1 HRTEM image of Ag crystals filled in a carbon nanotube.[35] Reprinted with permission from ref. 35. Copyright 1996, American Chemical Society.

 This journal is © The Royal Society of Chemistry 2008

nanocatalysts, is not often successful at atmospheric pressure yet even if low surface tension liquids such as ethanol and isopropanol have been used.[36] This is due to effects such as wall characteristics, interaction of the liquid with the wall, and the dynamics of wetting and filling in small pores.[17,31] A recent interesting study reported by Khlobystov *et al*. showed that fullerenes can be carried into nanotubes using supercritical CO_2 as a medium, which has no surface tension, very low viscosity and high diffusivity.[11] This has been achieved by immersing a mixture of nanotubes and fullerenes into the fluid under 100–150 kbar pressure.

In addition, the channels of the opened CNTs are usually filled with air, which opposes the entry of solution into the channels.[31,36] So does amorphous carbon inside tubes, which usually forms during CNT growth but cannot be completely removed during purification. For example, Ajayan *et al*. found it very difficult to fill open tubes with the low surface tension liquid lead even under vacuum in the absence of oxygen.[32] No filling was observed but the peripheries of the open tube ends seemed to become decorated with metals.

Furthermore, the transport resistance the liquid encounters within several micrometer long channels of CNTs cannot be neglected, which may also hinder filling. Likewise, long channels will cause transport resistances for reactants and products if the reaction takes place inside nanotubes. Thus shorter CNTs with better wetting properties are preferred for filling of catalysts and for catalytic reactions. For this purpose, we have developed a novel pre-treatment process, which includes purification, surface decoration and controlled cutting of nanotubes to a desired length.

2.2 Purification and cutting of CNTs

Scheme 1 describes the process we have developed for pre-treatment of CNTs in order to facilitate homogeneous dispersion of nanocatalysts inside nanotubes.[37] Pristine CNTs usually have closed ends and contain impurities such as residual catalysts and amorphous carbon, which have formed during CNT growth and need to be removed prior to deposition of catalysts. Treatment in *e.g*. concentrated nitric acid is a well practised process, which does not only purify CNTs but also opens their caps.[31,34–36] Furthermore, carboxylic, carbonyl and hydroxyl groups are introduced on their surfaces, which provide nucleation sites for subsequent deposition of metal species.[31,38] In addition, the resulting CNTs become more wettable in polar solvents such as water, which will facilitate the following filling of the channels using wet chemistry methods.

Many efforts have been made previously to cut long nanotubes. For example, AFM tips have been successfully used for cutting individual CNTs.[39] Similarly, a single-walled CNT (SWNT) bundle has been cut with a TEM electron beam.[40] Multi-walled CNTs (MWNTs) can be cut by ball milling, but this usually takes a rather long time *e.g*. over 10 h to obtain tubes shorter than 1 μm.[41] Cutting can also be achieved *via* oxidation of CNTs, *e.g*. by reaction with a large amount of NiO at 900 °C, with air at 600 °C or a concentrated H_2SO_4–HNO_3 mixture.[42–44] However, direct oxidation with air and in concentrated acid solution are not easy to control and they often lead to a significant weight loss. Recently, a method using a so-called piranha solution with 4 : 1 vol. ratio of 96% H_2SO_4–30% H_2O_2 was reported for cutting of SWNTs at room temperature, which resulted in a rather small weight loss (~15%).[45] We have previously treated our CNTs by refluxing them in 68% HNO_3 at 120 °C, resulting in 0.7–1.2 μm long nanotubes and a weight loss around 40%. The weight loss became greater if we wanted to cut nanotubes shorter. Therefore we decided to develop a process to control cutting of long MWNTs *via* catalytic oxidation with reduced losses.[37]

Ag was used as catalyst for oxidative cutting since it is known to catalyze oxidation of hydrocarbon compounds.[46] CNTs were impregnated with $AgNO_3$ followed by decomposition to Ag at 300 °C in Ar. Thus Ag particles formed with a particle size of 10–15 nm on the CNT exterior surfaces. Catalytic oxidation of Ag/CNTs was carried out in a 5 vol% O_2–Ar stream. Small pits formed around the positions where the catalyst particles were located due to oxidative etching of carbon. The subsequent ultrasound treatment in diluted nitric acid solution (2 M) removed the Ag catalysts and completed the breaking of nanotubes around the pits. Since oxidation caused a loss of CNTs, care was taken to choose suitable oxidation conditions, *i.e*. temperature and duration, which were sufficient to achieve cutting and yet not too severe to lose too many CNTs. The weight loss is usually around 20%.[37]

The length of nanotubes can be controlled by varying the loading of Ag. Fig. 2 shows that over 80% tubes are 200–500 nm long when the Ag loading is 5 wt% and oxidized for 105 min at 300 °C. With 2 wt% Ag, the resulting nanotubes are longer after cutting. Around 65% tubes are in the range of 500 nm to 1.0 μm. Further decreasing the Ag loading to 0.5 wt%, most of the tubes are longer than 1.5 μm.

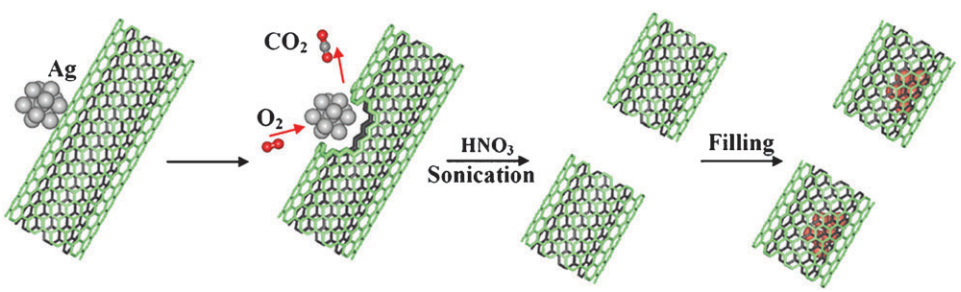

Scheme 1 Controlled cutting of CNTs and filling of nanocatalysts.[37]

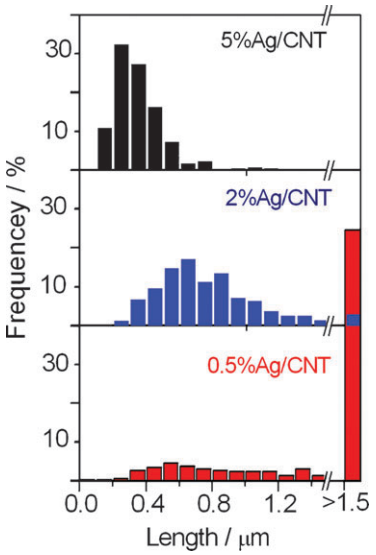

Fig. 2 Length distribution of CNTs after oxidation catalyzed by Ag/CNT with a varying Ag loading.[37]

2.3 Homogeneous dispersion of catalyst nanoparticles inside tailor-made CNTs

Oxidatively cut CNTs discussed above are short and opened, and their surfaces are decorated with oxygen containing groups. They can be readily wet by hydrophilic solvents. Therefore, we used a wet chemistry method for introducing metal nanoparticles inside CNTs. Considering the difficulties encountered previously during filling small nanotubes,[17,31,36] ultrasonic treatment and extended stirring were employed to aid the capillary actions. Using this method, iron oxide, rhodium and ruthenium nanoparticles have been introduced inside the CNT channels at a rather high efficiency.[23,24,37]

Taking filling of ruthenium as an example, acetone was chosen as a solvent for $RuCl_3$ since its surface tension (26 mN m^{-1}) is far below the cut-off value for wetting CNTs.[37] CNTs with 4–8 nm inner diameter were immersed in $RuCl_3$/acetone solution, which was subjected to ultrasonic treatment and extended stirring. This facilitated expulsion of the air out of the CNT channels. Thus the solution could migrate into the channels. In addition, extended stirring allowed slow evaporation of acetone outside of the nanotubes. Driven by the increasing concentration gradient more $RuCl_3$ entered the channels during this process. Following drying and reduction in H_2 for 5 h at 450 °C Ru/CNTs were obtained. From visual inspection of the sample under TEM, one can see that most particles (over 80%) have been introduced in CNTs. The particles are fairly uniform and most of them are in a range of 2–4 nm, which leaves sufficient space for diffusion of reactants and products in and out of the channels. This contrasts to earlier filling studies where the inner part of the CNT channels was almost completely blocked with *e.g.* NiO and Ag nanorods and particles.[34,35] Fig. 3 shows TEM images of such a composite material at different magnifications. Rotating the specimen under the microscope in two directions with respect to the electron beam confirmed the location of the majority of the particles inside the CNT channels.[37]

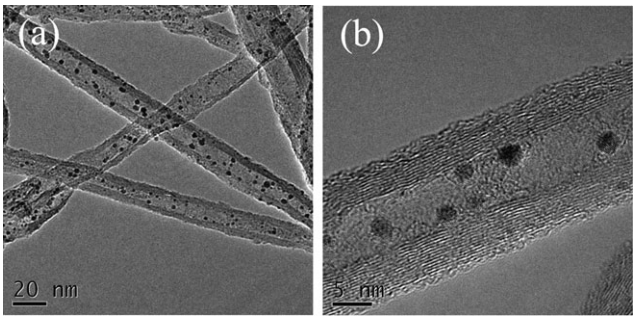

Fig. 3 TEM images of Ru nanocatalysts homogeneously dispersed inside the CNT channels at different magnifications.[37]

2.4 Dispersion of catalyst nanoparticles on the exterior surfaces of opened CNTs

In order to understand better the effect of confining nanocatalysts inside the CNT channels, it is essential to obtain a catalyst for comparison with metal particles dispersed exclusively on the CNT exterior surfaces. An easy way to achieve this goal is to use the nanotubes with closed ends, as shown in our previous studies.[23,24] However, the closed CNTs may exhibit different characteristics from the shortened and opened nanotubes concerning purity, surface area and different amount of surface oxygen groups due to different pretreatment they have gone through. This could affect the dispersion and the properties of metal catalysts, and hence the catalytic performance. Therefore it is desirable to use the same opened CNTs for inside and outside deposition of metal catalysts. However, the short and opened CNTs can be partially filled with the metal precursor solution because of the capillary actions. Thus, the ingress of catalyst particles cannot be avoided following standard wet chemistry procedures.

Therefore, it is vital to block the CNT channels temporarily so that only the exterior surfaces of opened CNTs are decorated with metal species. We first filled the CNT channels with an organic solvent *e.g.* xylene, which is immiscible with the solvent for $RuCl_3$ here (water). This prevented $RuCl_3$/water from infiltrating the channels when aqueous $RuCl_3$ solution was added. In the presence of $NH_3{\cdot}H_2O/NH_4HCO_3$, the xylene-filled CNTs transferred into and were well dispersed in $RuCl_3$ aqueous solution. The higher boiling point of xylene allowed the preferential evaporation of water on the outside of CNTs. Consequently, ruthenium deposited on the CNT exterior surface while the channels remained occupied by xylene. Then xylene was removed by further drying. Fig. 4 shows that

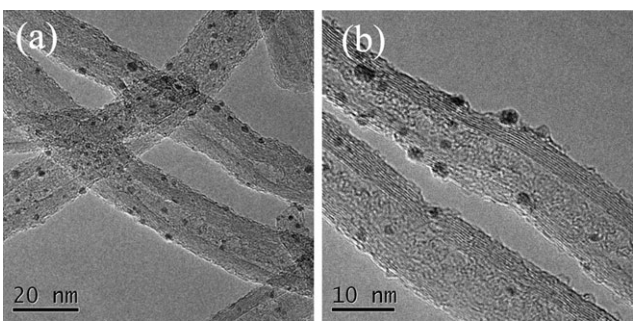

Fig. 4 TEM images of Ru particles dispersed on the exterior surfaces of opened CNTs at different magnifications.[37]

This journal is © The Royal Society of Chemistry 2008

most particles are well distributed on the CNT exterior surfaces in the resulting sample and their sizes are rather uniform (2–5 nm). Rotating the specimen under the electron microscope confirms the outside locations of Ru particles.[37]

These processes for the selective dispersion of nanoparticles inside or outside of CNTs are applicable to many other metals and metal oxides and thus provide the basis for further experimental studies of the CNT confinement in catalysis.

3. Redox properties of nanomaterials confined inside CNTs

Transition metals are known to interact with graphite through hybridization of their d orbitals with carbon p_z orbitals.[22] The deformation of sp^2 hybridization in the graphene walls causes π electron density to shift from the concave surface to the convex surface.[2,3,16–18] The contour plot in Fig. 5 shows the charge density for a (6,0) nanotube, which has been obtained from a theoretical study.[47] Thus a different electron potential forms inside and outside of CNTs. When a transition metal is placed in the CNT interior, it should interact with the graphene surface in a different way from that located on the CNT exterior. Theoretical studies have suggested a small charge transfer between transition metal atoms and SWNTs,[22,48,49] although there is yet little experimental evidence for such an interaction. Therefore we turned our attention first to the redox behavior of CNT-encapsulated model Fe catalysts.

3.1 Reduction of iron oxide inside CNTs

We introduced iron oxide nanoparticles into the CNT channels (inner diameter of 4–8 nm, outer diameter of 10–20 nm) and studied their reduction properties in comparison to those dispersed on the exterior surfaces of CNTs.[20,21] Iron oxide is known to be reducible by carbon at high temperatures giving CO and metallic iron as products. The same happened to Fe_2O_3 confined inside CNTs but they were reduced by CNTs (eqn (1)).

$$Fe_2O_3 + CNTs \rightarrow Fe + CO \qquad (1)$$

We observed that the reduction of Fe_2O_3 nanoparticles was significantly facilitated inside CNTs compared to those on the outside. *In situ* HRTEM indicated that the CNT-confined Fe_2O_3 particles transformed to metallic iron at 600 °C while

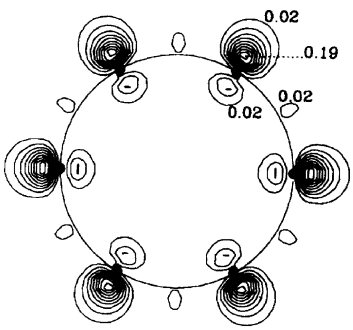

Fig. 5 Contour for the charge density of a (6,0) tube in a plane perpendicular to the tube axis with the circle representing a cross section where six carbon atoms are located.[47] Reprinted with permission from ref. 47. Copyright 1994, American Physical Society.

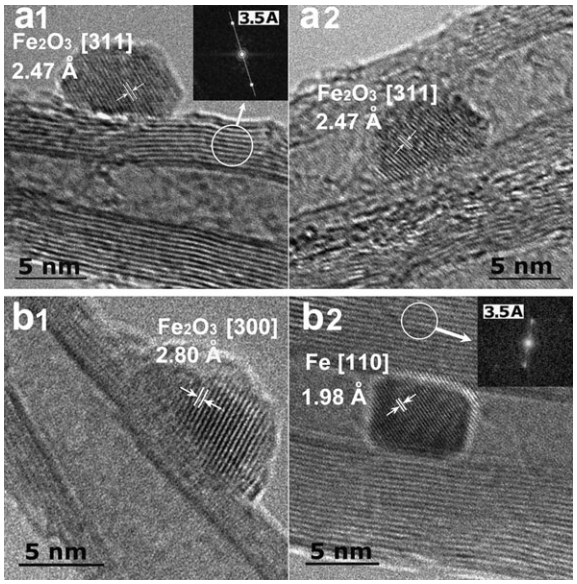

Fig. 6 *In situ* HRTEM images of Fe_2O_3/CNTs at (a) 20 °C and (b) 600 °C. (a1) and (b1) show outer while (a2) and (b2) inner particles with typical crystal planes.[20] Reprinted with permission from ref. 20. Copyright 2006, American Chemical Society.

the outside particles remained oxidic at this temperature (Fig. 6).[20] Note that the particle size in both samples was comparable. Temperature programmed reaction in inert gas showed that the reduction temperature of the outside iron oxide was 800 °C and confirmed the reduction at 600 °C for the inside particles. Interestingly, the reduction temperature of the confined Fe_2O_3 decreased with the inner diameter of CNTs. As demonstrated in Fig. 7, inside CNTs with an inner diameter of 2–5 nm the reduction of Fe_2O_3 took place at 584 °C but only at 620 °C for that inside 8–12 nm inner diameter nanotubes. This was further confirmed by *in situ* XRD and Raman spectroscopy.[21] A similar effect was recently reported for Fe_3O_4 nanowires, which were reduced to metallic iron inside CNTs at 570 °C, in comparison to reduction of

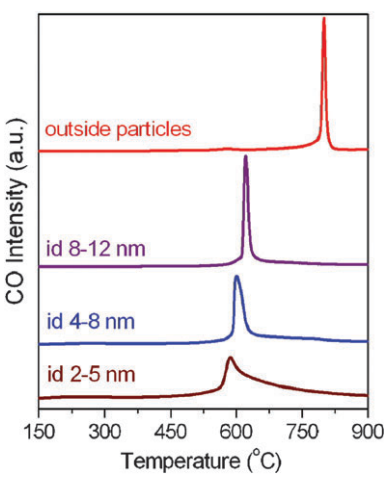

Fig. 7 Reduction behaviour of Fe_2O_3 confined in CNTs with a varying diameter in comparison to that on the exterior surface.[21] Reprinted with permission from ref. 21. Copyright 2007, American Chemical Society.

powdered Fe_3O_4 mechanically mixed with CNTs at a temperature higher than 700 °C.[50]

3.2 Oxidation of metallic iron particles inside CNTs

Oxidation of metallic Fe nanoparticles confined inside CNTs (inner diameter 4–8 nm) was found to be retarded in comparison to that of outside Fe particles, as shown by *in situ* XRD and gravimetric measurements with an online microbalance.[21] The overall activation energy for oxidation of the inside Fe was estimated to be 18 and 14 kJ mol^{-1} for the outside Fe particles, in comparison to 32 kJ mol^{-1} for bulk Fe.[21,51]

In order to separately evaluate the impact of the spatial restriction, SBA-15 and an activated carbon (XC-72) were chosen as supports for comparison. SBA-15 is a siliceous material with a periodic pore structure with an average diameter 6–7 nm and a pore length 300–600 nm. Thus it is comparable to the channel morphology of CNTs used here (inner diameter of 4–8 nm and length of 200–500 nm). It should offer a similar dimensional confinement for iron. XC-72 is a commercial carbon with a surface area (237 $m^2\ g^{-1}$) similar to CNTs (228 $m^2\ g^{-1}$) and a rather high degree of graphitization. Thus XC-72 provides a good comparison to CNTs, in particular to the case of the CNT outer surface. The results showed that the oxidation temperature of Fe particles increased in the following order: inside SBA-15 channels < on XC-72 ≈ on outer surface of CNTs < inside CNT channels.[21] A much faster oxidation rate of Fe particles in SBA-15 than in CNTs indicates that the oxygen diffusion into the CNT channels is not the main cause for the retarded oxidation of confined iron. The interaction of iron with the interior surfaces of CNTs likely plays a more important role.

Su *et al*. recently also observed a relatively high degree of reduction and good stability of Ru nanoparticles against oxidation, which were partially encapsulated inside the pores of a mesoporous carbon.[52] That carbon was synthesized using SBA-15 silica as a template and it has an inverse replica structure. Those authors also attributed the modified redox behavior to the interaction of Ru with the pore walls of carbon.

3.3 Characterization of the interaction of iron and iron oxide with CNT surfaces

The interaction of the confined iron oxide with CNTs was characterized by Raman spectroscopy (Fig. 8).[21] A red-shift of the most intense E_g Fe–O band was observed for the Fe_2O_3 nanoparticles on the outer CNT walls with respect to bulk Fe_2O_3, in agreement with the general observation for Fe_2O_3 nanoparticles in earlier reports.[53,54] However, this frequency shift was reversed when the Fe_2O_3 particles were moved from the exterior to the interior of 8–12 nm inner diameter CNTs. It further blue-shifted when the inner diameter became smaller. Although the particle size declined accordingly with the downsized CNT channels, the stepwise blue-shift of the Fe–O band here does not line up with the red shift generally reported for nanosized Fe_2O_3,[53,54] implying the presence of an interaction of the Fe_2O_3 particles with the inner CNT surface. Furthermore, this interaction becomes stronger within smaller CNTs.

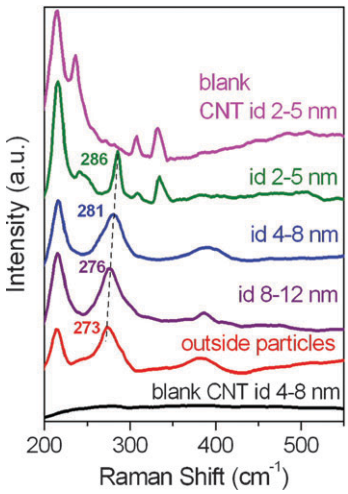

Fig. 8 Fe–O Raman band of Fe_2O_3 confined in CNTs with a varying diameter.[21] Reprinted with permission from ref. 21. Copyright 2007, American Chemical Society.

Therefore the distinct redox behavior of the interior Fe_2O_3 and Fe compared to the exterior ones can be at least partially attributed to the electronic interaction between metals and the CNT concave and convex surfaces. Inside smaller nanotubes the interaction between metals and graphene surfaces could become stronger since the sp^2 hybridization is more severely deformed. This can explain the more facile reduction of iron oxide inside smaller nanotubes.[21] Su *et al*. also attributed the impeded oxidation of Ru particles inside the pores of mesoporous carbon to the electronic interaction of Ru with curved graphene surfaces analogous to the CNT interior.[52]

Modification of the redox properties of metal particles inside CNTs may be a general characteristic. It can be exploited in catalysis, in particular for reactions which are sensitive to the electronic state of metal species. For example, hydrogen involving reactions *e.g*. syngas conversion, ammonia synthesis and catalysis in fuel cells are known to require reduced metals as catalysts. Furthermore, reduced transition metals can enhance the hydrogen adsorption/desorption capability of CNTs, which themselves have also been extensively studied as hydrogen storage materials.[55] Together these unique features may facilitate particularly hydrogen involving reactions over CNT-confined catalysts.

4. Tuning the catalytic activity of CNT-confined nanocatalysts

4.1 Reactions without additional catalysts inside CNTs

Several theoretical studies have suggested that chemical reactions can be influenced by confinement inside CNT channels alone. This is attributed to the significantly reduced reaction volume, and the interaction of reactants and products with the internal surface of CNTs.[56–58] For example, the D and H_2 exchange reaction to form HD and H has been predicted to be enhanced considerably inside CNTs compared to the gas phase.[56] Furthermore the reaction probabilities were considerably higher inside smaller CNTs. This enhancement was attributed to be steric in nature, having to do with the

This journal is © The Royal Society of Chemistry 2008

alignment of the H_2 along the tube axis. Another theoretical study suggested that the isomerization of *n*-butane, 1-butene and 1,3-butadiene should be significantly modified due to the steric hindrance inside CNTs with a pore size comparable to the molecules dimensions.[57]

CNTs are known to possess large electronic polarizability and thus the interaction with dipolar species may also affect reactions. One typical example is the Menshutkin S_N2 reaction, where two neutral molecules, NH_3 and CH_3Cl, combine to give a charged product $[H_3NCH_3]^+[Cl]^-$. Theoretical calculations suggested that dipolar species confined within nanotubes can interact with them *via* an induced image dipole on the CNTs.[58] Thus, the product species are stabilized inside CNTs with a significantly reduced reaction volume relative to the gas phase, making the overall reaction more favorable. For example, the reaction endothermicity is reduced by more than 23 kcal mol^{-1} within the (9,0) nanotubes. The activation energy is also significantly reduced compared to that in the gas phase.

Santiso *et al*. also predicted from theoretical studies using the reactive Monte Carlo (RxMC) method that the equilibrium of chemical reactions can be influenced inside the CNT channels.[15] For instance, they suggested that the yield of ammonia synthesis is enhanced compared to that in the gas phase largely due to the selective adsorption of ammonia inside CNTs.

An interesting experimental study was recently carried out by Kondratyuk and Yates on the reaction between 1-heptene and hydrogen atoms.[13] They demonstrated that the reactivity can be suppressed in the interior of SWNTs due to the nanotube walls shielding heptene molecules from the reactive atomic H species. Thus a kinetic hurdle is created for the incoming molecule: finding the point of entry into the nanotube, entering the nanotube, and diffusing inside the nanotube to react with the adsorbate there.

However, chemical reactions over nanocatalysts confined inside the CNT channels can be expected to exhibit a different behavior not only because of the space restriction, and interaction of reactants and products with the CNT walls, but also because of the modified redox properties of metal catalysts inside CNTs.

4.2 Reactions over nanocatalysts confined inside CNTs

4.2.1 Early studies. Only few studies have been carried out over catalysts confined inside CNTs so far. For example, Zhang *et al*. deposited a $HRh(CO)(PPh_3)_3$ complex catalyst on opened and closed CNTs, respectively, for hydroformylation of propene.[59] The reaction gave a turnover frequency (TOF) of 0.10 s^{-1} and molar ratio of the normal/branched product (n/i) = 9 over the opened nanotube catalyst in comparison to a TOF of 0.06 s^{-1} and (n/i) = 6.0 over the closed CNT catalyst. The authors proposed that the CNT channel size ~3–4 nm fitted well with the size of Rh complexes (~1.8 nm) and thus favored the regioselectivity to reaction intermediates of the product butylaldehyde due to the spatio-restraint.[59] In addition, they proposed that the delocalized valence electrons of the graphene layer of CNTs interacted with the phenyl rings of PPh_3 ligands and thus might favor electron donation from the coordinated PPh_3 ligands to Rh, which could also help improving the activity by comparison to catalysts supported on other porous materials *e.g*. SiO_2 and activated carbon.[59] Although no direct evidence was provided about the exact location of Rh catalysts over the opened CNTs, one can assume that at least part of the Rh complexes were inside the channels in comparison to the catalyst over the closed nanotubes.

In another study Pd particles were introduced inside CNTs with an inner diameter of 5–10 nm for benzene hydrogenation.[60] The TOF of benzene was double of that over Y zeolite and activated carbon supported catalysts although Y and AC have much higher specific surface areas than CNTs. The authors attributed this enhancement to the large pore diameter and the capillary action of nanotubes, which benefited the wetting and conversion of the liquid reactant.

CNTs with an average inner diameter of 40 nm were also used to confine Pd particles as catalysts for liquid phase selective hydrogenation of cinnamaldehyde.[61] The conversion was similar to that over activated carbon supported catalysts, but the selectivity differed significantly. Only 10% fully hydrogenated alcohol was obtained and the rest was the aldehyde with selective C=C hydrogenation on the CNT catalyst, while on the activated carbon catalyst these two products were in equal proportion.

Nhut *et al*. deposited Ni_2S inside CNTs with an inner diameter of 50–80 nm (Fig. 9(a)) and used it as a catalyst for oxidation of H_2S to form S and H_2O.[62] The confined Ni_2S exhibited an enhanced activity compared to an SiC grain-supported catalyst. The authors attributed this to the surface characteristics of CNTs. They argued, based on the evidence from TEM images shown in Fig. 9(b), that water produced from the reaction condensed inside tubes, which washed the solid sulfur from the active site on the inner surface to the outside of CNTs. Consequently the catalyst deactivation due to sulfur plugging was alleviated with respect to purely hydrophobic or hydrophilic supports such as SiC, graphite or alumina.[62]

4.2.2 Local concentration of CO and H_2 inside CNTs. Recently, we have begun to study syngas conversions over catalysts confined in CNTs to liquid fuels and oxygenates

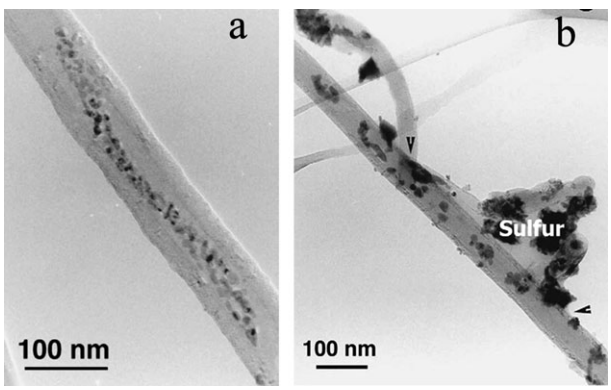

Fig. 9 TEM image for Ni_2S encapsulated inside the CNT channels (a) before reaction; (b) after reaction.[62] Reprinted with permission from ref. 62. Copyright 2003, Elsevier.

which are considered to be promising routes for utilization of coal, natural gas and biomass. As the first step we did simulations on the local concentration of CO and H_2 inside CNTs because that could play a role in the reaction.[63] First-principle and Monte Carlo calculations show that both CO and H_2 molecules have higher binding energies in the CNT interior than on the exterior. This is in agreement with similar findings of Kondratyuk and Yates.[13] They looked at different binding sites in SWNTs: the nanotube interior and exterior surface, and the groove sites on the outside of the bundles where a pair of nanotubes meet. They observed that the binding strength of different adsorption sites for molecules such as CF_4 and 1-heptene exhibited a hierarchy, interior > groove > exterior sites.

Due to the higher binding energies of CO and H_2 molecules in the CNT interior,[63] they are enriched inside the channels with respect to the outside (Scheme 2) when CNTs are placed in the CO and H_2 atmosphere. This enrichment becomes greater inside smaller nanotubes. The increased local concentration of reactants could help accelerate the reaction rate.

4.2.3 Fischer–Tropsch synthesis (FTS) to liquid fuels. Syngas conversion *via* FTS was chosen as a probe reaction because its activity is known to be related to the structural and electronic properties of the catalysts.[23,64] In particular, formation of carbides is deemed to be essential to obtain high FTS activity. Fig. 10(a) shows that the CO conversion over the encapsulated iron catalyst (shown as bars with filled patterns) was almost 1.5 times that over the outside iron catalyst (empty bars).[23] The confined catalyst favored selective conversion to long chain hydrocarbons, for example those containing five and more carbon atoms (expressed as C_{5+}). Thus the yield of C_{5+} hydrocarbons was twice that over the outside catalyst. Furthermore, the yield was six times higher than that over iron supported on the XC-72 activated carbon with similarly high surface area.

Characterization of the catalysts by TPR both in H_2 and CO showed a significant difference in the reducibility.[23] Fe_2O_3 was reduced stepwise in H_2, first converted to FeO and then to metallic Fe. Each reduction step for the confined catalyst occurred at a temperature *ca* 100 °C lower than that for the outside catalyst regardless of the reducing agent. This is

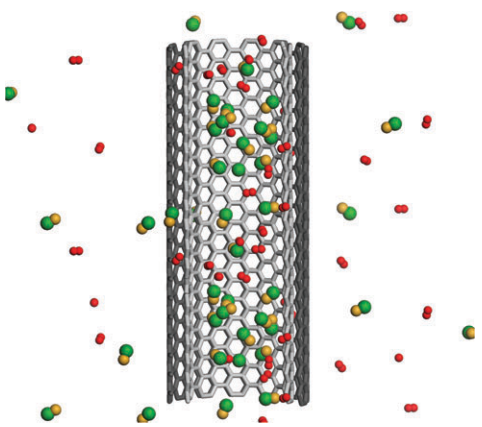

Scheme 2 Schematic description for CNT-induced CO and H_2 distribution inside and outside the channels.

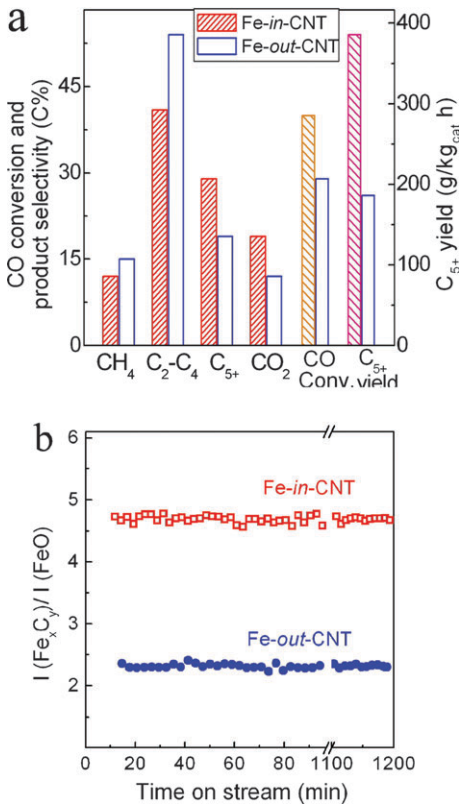

Fig. 10 (a) FTS activity of Fe-*in*-CNT and Fe-*out*-CNT at 280 °C and 50 bar. (b) Comparison of the iron carbide/iron oxide ratio at 9 bar.[23] Reprinted with permission from ref. 23. Copyright 2008, American Chemical Society.

remarkable considering that the diffusion of H_2 or CO in CNTs may slow down the reaction to a certain extent inside with respect to that on the freely accessible CNT outer surfaces. It indicates that the reducibility of the CNT-encapsulated iron oxide has been significantly improved. This should favor the formation of iron carbide under reaction conditions.

This was confirmed by *in situ* XRD characterization when iron was exposed to syngas under FTS conditions.[23] As shown in Fig. 10(b), the CNT confined iron catalyst exhibited an obviously higher iron carbide/iron oxide ratio in comparison to the outside catalyst. This was due to the interaction of metallic iron with dissociated CO. The improved reducibility favored formation of more iron carbides. A monotonic correlation between the carburization extent and the activity had been frequently observed in earlier studies using XRD and Mössbauer spectroscopy.[65,66] Therefore, the higher syngas conversion activity obtained over the CNT-confined iron catalyst can be at least partly attributed to its higher carbide content due to better reducibility.

4.2.4 Syngas conversion to C_2 oxygenates. Another reaction we looked at was syngas conversion to C_2 oxygenates such as ethanol, acetic acid and acetaldehyde, which is known to be catalyzed by reduced Rh. Mn is often used as an additive to promote the conversion and selectivity to oxygenates. Therefore, a bicomponent Rh–Mn catalyst was introduced into the CNT channels (Fig. 11(a)).[24] A remarkable

This journal is © The Royal Society of Chemistry 2008

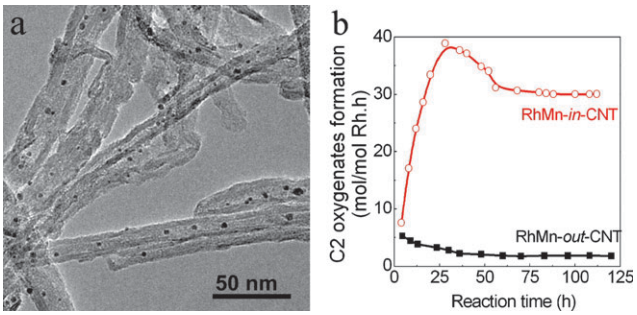

Fig. 11 (a) TEM image of the CNT confined bicomponent RhMn catalyst. (b) Activity of RhMn-*in*-CNT and RhMn-*out*-CNT in syngas conversion at 320 °C and 30 bar.[24]

enhancement of the catalytic activity was observed compared to the catalyst with RhMn dispersed on the CNT exterior surfaces (Fig. 11(b)). Again SBA-15 was chosen as a support for comparison and again the SBA-15 supported catalyst exhibited a much lower activity under the same reaction conditions.[24]

Characterization of the catalysts with TEM showed that the small channels of CNTs had effectively prevented the sintering of metal particles during reaction. For example, the fresh confined Rh–Mn catalyst had a particle size 1–2 nm. They grew to 4–5 nm after 120 h reaction time on stream, which fell in the range of the CNT internal diameter (4–8 nm).[24] In comparison, the outside RhMn catalyst had a particle size of 2–3 nm prior to reaction and 5–8 nm after reaction, which was not significantly larger than that of the confined catalyst. However, the catalytic activity was by far lower than that of the inside catalyst. Therefore, the particle size cannot be the only factor determining the catalytic activity here.

Raman spectroscopic charaterization of the CO-adsorbed catalysts indicated that the activation of CO likely was modified inside CNTs. When the reduced catalysts were exposed to CO at room temperature, two Raman bands corresponding to the Rh–C and Mn–O bonds were observed on the confined catalyst whereas only the Rh–C band appeared on the outside catalyst.[24] This can be explained again by the interaction of the metals with CNTs.

RhMn in the CNT interior likely exists in a more reduced state than that on the exterior. When CO is adsorbed on Rh inside CNTs, the adjacent oxophilic Mn tends to attract the O of the adsorbed CO leading to tilted adsorption forming the Rh–C and Mn–O bonds. Such a tilted adsorption of CO facilitates the dissociation of CO, which improves the activity.[67,68] In contrast, the electronic structure of exterior CNT surface approaches a planar graphite layer since the outer diameter is around 10–20 nm. Thus the tendency of Mn to accept oxidic CO donor electrons could be reduced in comparison to that inside the electron-deficient interior of CNTs. Consequently, the CNT confined catalyst could exhibit a higher activity in CO conversion than the catalyst dispersed on the CNT exterior surfaces.

The above examples show that the catalytic behavior of the CNT confined iron and rhodium catalysts have been significantly modified in comparison to those dispersed on the CNT exterior surfaces and conventional porous materials such as activated carbon and silica. Characterization suggests that the interaction between metals and the graphene surfaces, and locally higher concentration of reactants inside the CNT channels may play important roles apart from the geometrical restriction on metal particle size.

Summary and perspective

This article summarizes recent advances in confining metal catalysts inside CNTs and reactions over them. The studies show that the CNT channels provide an intriguing confinement environment for nanocatalysts and catalytic reactions. In addition to the effect of spatial restriction on the metal particles and local concentration of reactants inside CNTs, the redox properties of metal catalysts are modified due to the interaction of the encapsulates with the interior CNT surfaces. For example, the reduction of metal oxides is facilitated inside CNTs with respect to those on the CNT exterior surfaces and the extent of facilitation depends on the CNT diameters. Also, the oxidation of CNT-confined metallic iron is retarded. Modification of the redox properties of incorporated catalysts is expected to be a general feature of CNTs. This provides a novel approach to tune the catalytic behavior of metal catalysts for reactions, which are sensitive to the electronic state of the active components, *e.g.* syngas conversion, hydrogenation/dehydrogenation of hydrocarbons, ammonia synthesis and catalysis in fuel cell (Scheme 3).

Currently experimental studies of the reaction over CNT-confined catalysts are essentially limited to MWNTs because they are easier to produce in a sufficiently large quantity than *e.g.* SWNTs and DWNTs. In addition, techniques for filling metal nanoparticles into MWNTs are more mature due to their relatively larger internal diameters. However, from the structural property point of view SWNTs and DWNTs are more interesting for this application because they have a higher degree of uniformity since they consist of only one or two graphene sheets with less defects. In addition, their diameter distribution is generally narrower (range of 1–3 nm), while the diameters of MWNTs are usually scattered over a much wider range. Furthermore, the carbon sp^2 hybridization becomes more deformed in SWNTs and DWNTs because of their large curvatures,[2,3,16–18] which could lead to a stronger interaction with metals. In contrast, the outer diameter of MWNTs is usually larger than 10 nm and the electronic

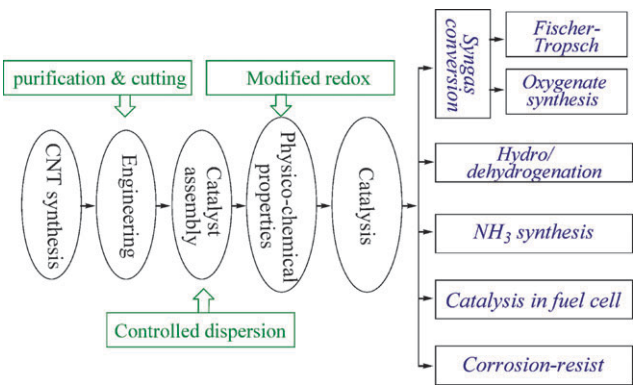

Scheme 3 A concept of tuning the properties of nanocatalysts and hence their catalytic behavior *via* confinement inside CNTs.

structure approaches that of a planar graphite layer. Therefore, confinement inside SWNTs and DWNTs is anticipated to have an even greater influence on the catalytic behavior. Studies on these even more simple catalyst-CNT systems may provide a deeper insight into the nature of the host–guest interaction and the catalytic behavior of thus confined nanocatalysts.

Another intriguing aspect of SWNTs is that they are either metallic or semiconducting with a different electron structure around the Fermi level.[2,3] Therefore metal catalysts may be modified in a different way by these two types of SWNTs. However, this requires selective synthesis of metallic and semiconducting SWNTs or efficient post-synthesis separation. This is currently under investigation but still limited to a very small scale.[69]

Looking into the future, the few examples discussed here show great promise and should stimulate further investigations on the effect of confining nanocatalysts inside CNTs. In particular, the understanding of the nature of these confined systems requires more advanced characterizations and theoretical studies on the interactions between metal particles, CNT surfaces and gas molecules as well as transport behavior of gas molecules inside such small channels.

Acknowledgements

The authors acknowledge the financial support from Natural Science Foundation of China (20503033 and 20573107) and the Ministry of Science and Technology (2006CB932703).

Notes and references

1 E. Auer, A. Freund, J. Pietsch and T. Tacke, *Appl. Catal., A*, 1998, **173**, 259.
2 H. Dai, J. H. Hafner, A. G. Rinzler, D. T. Colbert and R. Smalley, *Nature*, 1996, **384**, 147.
3 *Carbon Nanotubes Science and Applications*, ed. M. Meyyappan, CRC Press LLC, 2005.
4 J. M. Planeix, N. Coustel, B. Coq, V. Bretons, P. S. Kumbhar, R. Dutartre, P. Geneste, P. Bernier and P. M. Ajayan, *J. Am. Chem. Soc.*, 1994, **116**, 7935.
5 K. P. de Jong and J. W. Geus, *Catal. Rev. Sci. Eng.*, 2000, **42**, 481.
6 P. Serp, M. Corrias and P. Kalck, *Appl. Catal., A*, 2003, **253**, 337.
7 G. L. Bezemer, U. Falke, A. J. van Dillena and K. P. de Jong, *Chem. Commun.*, 2005, 731.
8 W. Li, C. Liang, J. Qiu, W. Zhu, H. Han, Z. Wei, G. Sun and Q. Xin, *Carbon*, 2002, **40**, 787.
9 W. M. H. Sachtler, *Acc. Chem. Res.*, 1993, **26**, 383.
10 J. Sun, D. Ma, H. Zhang, X. Liu, X. Han, X. Bao, G. Weinberg, N. Pfaender and D. Su, *J. Am. Chem. Soc.*, 2006, **128**, 15756.
11 A. N. Khlobystov, D. A. Britz and G. A. D. Briggs, *Acc. Chem. Res.*, 2005, **38**, 901.
12 J. Sloan, A. I. Kirkland, J. L. Hutchison and M. L. H. Green, *Acc. Chem. Res.*, 2002, **35**, 1054.
13 P. Kondratyuk and J. T. Yates, *Acc. Chem. Res.*, 2007, **40**, 995.
14 G. Chen, J. Qiu and H. Qiu, *Scr. Mater.*, 2008, **58**, 457.
15 E. E. Santiso, A. M. George, C. H. Turner, M. K. Kostov, K. E. Gubbins, M. Buongiorno-Nardelli and M. Sliwinska-Bartkowiak, *Appl. Surf. Sci.*, 2005, **252**, 766.
16 R. C. Haddon, *Science*, 1993, **261**, 1545.
17 D. Ugarte, A. Chatelain and W. A. de Heer, *Science*, 1996, **274**, 1897.
18 B. Shan and K. Cho, *Phys. Rev. B*, 2006, **73**, 081401.
19 Z. Peralta-Inga, P. Lane, J. S. Murray, S. Boyd, M. E. Grice, C. J. O'Connor and P. Politzer, *Nano Lett.*, 2003, **3**, 21.
20 W. Chen, X. Pan, M. G. Willinger, D. S. Su and X. Bao, *J. Am. Chem. Soc.*, 2006, **128**, 3136.
21 W. Chen, X. Pan and X. Bao, *J. Am. Chem. Soc.*, 2007, **129**, 7421.
22 M. Menon, A. N. Andriotis and G. E. Froudakis, *Chem. Phys. Lett.*, 2000, **320**, 425.
23 W. Chen, Z. Fan, X. Pan and X. Bao, *J. Am. Chem. Soc.*, 2008, **130**, 9414.
24 X. Pan, Z. Fan, W. Chen, Y. Ding, H. Luo and X. Bao, *Nat. Mater.*, 2008, **6**, 507.
25 C. Guerret-Piécourt, Y. Le Bouar, A. Loiseau and H. Pascard, *Nature*, 1994, **372**, 761.
26 S. Seraphin, D. Zhou, J. Jiao, J. C. Withers and R. Loutfy, *Appl. Phys. Lett.*, 1993, **63**, 2073.
27 L. Guan, Z. Shi, M. Li and Z. Gu, *Carbon*, 2005, **43**, 2780.
28 F. Stercel, N. M. Nemes, J. E. Fischer and D. E. Luzzi, *Mater. Res. Soc. Symp. Proc.*, 2002, **706**, Z7.8.1.
29 H. Shiozawa, T. Pichler, A. Grüneis, R. Pfeiffer, H. Kuzmany, Z. Liu, K. Suenaga and H. Kataura, *Adv. Mater.*, 2008, **20**, 1443.
30 E. Dujardin, T. W. Ebbesen, H. Hiura and K. Tanigaki, *Science*, 1994, **265**, 1850.
31 T. W. Ebbesen, *J. Phys. Chem. Solids*, 1996, **57**, 951.
32 P. M. Ajayan, T. W. Ebbesen, T. Ichihashi, S. Iijima, K. Tanigaki and H. Hiura, *Nature*, 1993, **362**, 522.
33 M. V. Chernysheva, A. A. Eliseev, A. V. Lukashina, Y. D. Tretyakova, S. V. Savilovb, N. A. Kiselevc, O. M. Zhigalinac, A. S. Kumskovc, A. V. Krestinind and J. L. Hutchison, *Physica E*, 2007, **37**, 62.
34 S. C. Tsang, Y. K. Chen, P. J. F. Harris and M. L. H. Green, *Nature*, 1994, **372**, 159.
35 A. Chu, J. Cook, R. J. R. Heesom, J. L. Hutchison, M. L. H. Green and J. Sloan, *Chem. Mater.*, 1996, **8**, 2751.
36 H. Ma, L. Wang, L. Chen, C. Dong, W. Yu, T. Huang and Y. Qian, *Catal. Commun.*, 2007, **8**, 452.
37 C. Wang, S. Guo, X. Pan, W. Chen and X. Bao, *J. Mater. Chem.*, 2008, DOI: 10.1039/b811560e.
38 R. Giordano, P. Serp, P. Kalck, Y. Kihn, J. Schreiber, C. Marhic and J. Duvail, *Eur. J. Inorg. Chem.*, 2003, 610.
39 J. Y. Park, Y. Yaish, M. Brink, S. Rosenblatt and P. L. McEuen, *Appl. Phys. Lett.*, 2002, **80**, 4446.
40 F. Banhart, J. Li and M. Terrones, *Small*, 2005, **1**, 953.
41 N. Pierard, A. Fonseca, Z. Konya, I. Willems, G. Van Tendeloo and J. B. Nagy, *Chem. Phys. Lett.*, 2001, **335**, 1.
42 X. X. Wang, J. N. Wang, L. F. Su and J. J. Niu, *J. Mater. Chem.*, 2006, **16**, 4231.
43 M. Q. Tran, C. Tridech, A. Alfrey, A. Bismarck and M. S. P. Shaffer, *Carbon*, 2007, **45**, 2341.
44 J. Liu, A. G. Rinzler, H. J. Dai, J. H. Hafner, R. K. Bradley, P. J. Boul, A. Lu, T. Iverson, K. Shelimov, C. B. Huffman, F. Rodriguez-Macias, Y. S. Shon, T. R. Lee, D. T. Colbert and R. E. Smalley, *Science*, 1998, **280**, 1253.
45 K. J. Ziegler, Z. N. Gu, H. Q. Peng, E. L. Flor, R. H. Hauge and R. E. Smalley, *J. Am. Chem. Soc.*, 2005, **127**, 1541.
46 A. Palermo, A. Husain, M. S. Tikhov and R. M. Lambert, *J. Catal.*, 2002, **207**, 331.
47 X. Blase, L. X. Benedict, E. L. Shirley and S. G. Louie, *Phys. Rev. Lett.*, 1994, **72**, 1878.
48 Y. Yagi, T. M. Briere, M. H. Sluiter, V. Kumar, A. A. Farajian and Y. Kawazoe, *Phys. Rev. B*, 2004, **69**, 075414.
49 D. M. Duffy and J. A. Blackman, *Phys. Rev. B*, 1998, **58**, 7443.
50 F. Cao, K. Zhong, A. Gao, C. Chen, Q. Li and Q. Chen, *J. Phys. Chem. B*, 2007, **111**, 1724.
51 A. P. Grosvenor, B. A. Kobe and N. S. McIntyre, *Surf. Sci.*, 2005, **574**, 317.
52 F. Su, L. Lv, F. Y. Lee, T. Liu, A. I. Cooper and X. S. Zhao, *J. Am. Chem. Soc.*, 2007, **129**, 14213.
53 D. L. A. de Faria, S. V. Silva and M. T. de Oliveira, *J. Raman Spectrosc.*, 1997, **28**, 873.
54 F. J. Owens and J. Orosz, *Solid State Commun.*, 2006, **138**, 95.
55 H. Kim, H. Lee, K. Han, J. Kim, M. Song, M. Park, J. Lee and J. Kang, *J. Phys. Chem. B*, 2005, **109**, 8983.
56 T. Lu, E. M. Goldfield and S. K. Gray, *J. Phys. Chem. C*, 2008, **112**, 2654.
57 E. E. Santiso, M. B. Nardelli and K. E. Gubbins, *J. Chem. Phys.*, 2008, **128**, 034704.
58 M. D. Halls and H. B. Schlegel, *J. Phys. Chem. B*, 2002, **106**, 1921.

 This journal is © The Royal Society of Chemistry 2008

59 Y. Zhang, H. Zhang, G. Lin, P. Chen, Y. Yuan and K. R. Tsai, *Appl. Catal., A*, 1999, **187**, 213.
60 A. M. Zhang, J. L. Dong, Q. H. Xu, H. K. Rhee and X. L. Li, *Catal. Today*, 2004, **93–95**, 347.
61 J. Tessonnier, L. Pesant, G. Ehret, M. J. Ledoux and C. Pham-Huu, *Appl. Catal., A*, 2005, **288**, 203.
62 J. Nhut, L. Pesant, J. Tessonnier, G. Winé, J. Guille, C. Pham-Huu and M. Ledoux, *Appl. Catal., A*, 2003, **254**, 345.
63 J. Guan, X. Pan and X. Bao, unpublished work.
64 L. Guczi, G. Stefler, O. Geszti, Zs. Koppány, Z. Kónya, É. Molnár, M. Urbán and I. Kiricsi, *J. Catal*., 2006, **244**, 24.
65 G. B. Raupp and W. N. Delgass, *J. Catal*., 1979, **58**, 348.
66 H. Jung and W. J. Thomson, *J. Catal*., 1992, **134**, 654.
67 H. Trevino, G. Lei and W. M. H. Sachtler, *J. Catal*., 1995, **154**, 245.
68 M. Ichikawa and T. Fukushima, *J. Phys. Chem*., 1985, **89**, 1564.
69 R. Krupke, F. Hennrich, H. V. Loehneysen and M. M. Kappes, *Science*, 2003, **301**, 344.